Preparation for:

"A Rheological Study of Nano-Layered Silicates in an External Electric Field"

Author: Børge Aune Schjelderupsen

Supervisor: Prof. Jon Otto Fossum

December 17, 2006

Norwegian University of Science and Technology

Department of Physics

NTNU

Innovation and Creativity

Abstract

Suspensions of laponite, a synthetic smectite clay, dispersed in silicone oil show a dramatic increase in the viscosity under the influence of an electric field. This is an example of an electrorheological fluid. Here the general properties of the dispersions with and without an electric field are measured with a rheometer. The viscosity of the suspension as a function of volume fraction laponite added was fitted to the Krieger-Dougtherty expression, which gave a maximum packing fraction of 0.71. The stability of the dispersions was also investigated. I found that the concentration decrease over time due to particle sedimentation. The static yield stress of suspensions with different laponite concentrations in electric fields from 200 to 1000 $\frac{\mathrm{V}}{\mathrm{mm}}$ was also measured. It was found the the static yield stress τ_s depends on the volume fraction Φ and the electric field E, according to $\tau_s = \Phi^\beta \cdot E^\alpha$, where β was close to 1 and α was around 1.70, except for the lowest concentration where $\alpha = 2.37$.

An attempt to alter the surface properties of laponite was also made in order for the laponite to disperse as single particles in oil. By treating the clay with a quaternary ammonium surfactant (CTAB) the surfaces of the clay ought to be hydrophobic, or actually lipophilic. This attempt was not successful, partly because of insufficient grinding of the finished powder. Further attempts will be made in the future.

An industrial modified laponite clay dispersed in silicone oil was also investigated. This dispersion was more stable compared to the normal laponite suspension, but the static yield stress was much lower.

Preface

This report is the documentation of the project work done as a part of the specialization course TFY4705 in the study for Master of Technology (norwegian: "sivilingeniør") at the Norwegian University of Science and Technology (NTNU), autumn 2006. The project work was performed at the group of Complex Materials at the Department of Physics with Prof. Jon Otto Fossum as supervisor.

The main focus of my work has been rheological studies of laponite clay particles suspended in oil under the influence of an external electric field. These systems show a dramatically increase in the viscosity when the electric field is high enough, indicating a transition from a liquid to a solid like state. The effect is known as the electrorheological effect. For me it has been interesting to get insight into new disciplines such as rheology and electrorheology.

I would like to thank my supervisor Prof. Jon Otto Fossum for all the help and support he gave during the work. I would also like to thank PhD. K.P.S Palmar for taking the time to help me getting started with the rheometer, my colleague in the dangerous chemistry work Svein Åsmund Slungård, research scientist Ahmed Gmira for helping us with the surface modification of laponite and all the other students at the lab.

Trondheim, December 17, 2006 Børge Aune Schjelderupsen

Contents

1 Motivation and Outline

In this project I have worked with rheological measurements on laponite, a synthetic smectite clay, dispersed in silicone oil. This dispersion is an example of an electrorheological (ER) fluid. PhD. K.P.S Palmar discovered a strange behavior of the static yield stress for these suspensions in low electric fields (less than 1 $\frac{\text{kV}}{\text{mm}}$) during his Phd. work[1]. My goal was to try to find out more about the behavior of the ER-fluid in this low field region, but also some general properties of the suspensions without an electric field present. I have also done some work together with Svein Åsmund Slungård, to try to alter the surface properties of the laponite clay in order to improve the stability of the dispersions.

The report is organized in two parts. In **Part I** I will discuss the rheological properties of dispersions of laponite in silicone oil, with and without electric field present. First I will give a brief introduction to the field of electrorheology. In Chapter 3 I will present the theory used, which include some general concepts used in rheology, rheology of suspensions, some simple models used to describe the electrorheological effect and flow behavior of ER fluids. Chapter 4 contains information about the materials used and experimental setup and measurements. The results and analysis are presented in Chapter 5, while a summary and conclusion is given in Chapter 6.

Part II of this report contains the work that has been done in collaboration with Svein Åsmund Slungård. First I will give a brief introduction to clays in water and ionic exchange. Then I will describe the procedure we used together with some measurements done with the rheometer. The results of rheological measurements on an industrial modified laponite clay in silicone oil will also be presented.

Part I

Rheology of Laponite Dispersed in Silicon Oil

2 Introduction to Electrorheology

An electrorheological fluid is a fluid which can switch over to a solid-like state upon application of an electric field typically in the order of $1\frac{\text{kV}}{\text{mm}}$. The transition can be observed both visually and by measuring the rheological properties (viscosity, yield stress, etc.). The ER effect is fast (order of milliseconds) and reversible, i.e. when switching of the electric field the suspension goes back to a liquid state.

The ER effect was first described by Winslow[2] in 1949, although the phenomenon had been observed already in the late nineteenth century. It was not until the 1980's the subject got a lot of attention and numerous scientific publications started to come out. This was when the industry discovered the potential of using ER fluids in industrial applications.

A typical ER fluid consists of colloid particles suspended in an insulating oil (forming a suspension), but also some emulsions (liquid in oil) are ER active. In this paper I will only discuss the former. When an electric field is applied the particles suspended in oil form fibrous, chain-like structures along the direction of the electric field. A generally accepted theory for this is that the electric field polarizes the particles, which in turn interact with each other forming chains. If the electric field and/or the dispersed particle concentration is high enough, chains can interact with each other forming thick column-like structures.

Insulating oils used to prepare ER fluids are silicone oil, vegetable oil, mineral oil, paraffin, kerosene, chlorinated hydrocarbons, transformer oil etc. An ideal dispersing liquid should have low volatility, high chemical stability, high boiling point, low viscosity, high brake down strength, relative high density and a low dielectric constant. A wide range of solid particles can be used to make ER fluids: clays, organic and polymeric semiconducting materials, carbonaceous materials and fullerence and superconductive materials[3].

The particle size and shape have an impact on the ER effect. The ER effect is expected to be weak if the particles are to small, due to Brownian motion competing with fibrillation. Very large particles are also expected to show a weak ER effect because of particle sedimentation. Particle sizes from 0.1 to 100 μm are commonly used in the present ER fluids. The influence of particle size on the ER effect is quite diverse. However, when mixing particles of different sizes it is found that the ER effect decreases. Since the ER effect involves polarization of particles, it is quite likely that the shape of particles would have some effect on the magnitude of the response. Ellipsoidal particles are expected to give a stronger ER effect than spherical particles. Experiments on cylindrical fibers with different aspect ratios showed that the ER effect increased significantly with aspect ratio[4].

The main motivation for studying ER materials has been the possibility of using them in various industries, especially in the automotive- and robotics industry. The reason for this is that we can controll the state of the material by an electrical signal, making it a perfect mechanical-electrical interface. Proposed applications are ER clutches, brakes, damping devices, hydraulic valves, smart training equipment etc. Some of these applications have already been patented.

There are several challenges that must be overcome before ER fluids can be used for industrial applications. The main problem with the present ER fluids are the they have too low yield stress, i.e. they can not handle the stress needed for the industrial applications. The are also problems with the stability of the suspensions due to sedimentation. A decrease in the concentration gives a lower ER effect.

By understanding the mechanisms that control the ER effect better, we can choose the most suitable materials, both in terms of yield stress strength and stability. The properties of ER fluid can also be further improved by adding additives to the suspensions that enhances the ER effect and improves particle sedimentation properties.

3 Theory

3.1 Rheology

The term *rheology* was introduced by Professor Bingham of Lafayette College, Indiania, on the advice of a colleague. It means the *science of deformation and flow of matter*. This definition was accepted when the American Society of Rheology was founded in 1929.

Rheology deals with widely differing materials such as asphalts, lubricants, paints, plastics, rubber, polymers, cosmetics, food articles, suspensions and many more. This makes rheology a multidisciplinary discipline involving scientists with different backgrounds, such as physics, mathematics, chemistry, biology and engineering. Rheology has played a very important role in the chemical processing industry.

The definition of rheology suggest that the behavior of all matter can be studied, from Hookean solids to Newtonian viscous liquids. However, these two classical extremes are considered to be outside the scope of rheology. Nevertheless they are useful because they introduce important concepts and definitions used in rheology. I will give a brief introduction of the two cases in the following sections.

3.1.1 Hookean Solid

Lets consider a Hookean solid with the bottom face fixed, as shown in Figure 3.1. A force F is applied to the upper surface (area A). The resulting shear stress $\tau = \frac{F}{A}$, is given by

$$\tau = G\gamma, \tag{3.1}$$

where γ is the shear angle (strain) and G is the shear modulus.

3.1.2 Newtonian Liquids

Consider a liquid between two parallel planes (area A), shown in Figure 3.2. A force F gives the upper plane a velocity U. The shear stress required to produce the motion is

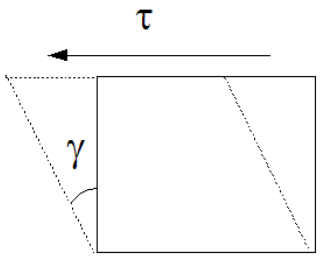

Figure 3.1: Hookean solid sheared at upper surface

$$\tau = \eta \frac{U}{d} = \eta \frac{\mathrm{d}v_x}{\mathrm{d}y} = \eta \dot{\gamma}, \tag{3.2}$$

where η is the shear viscosity or simply the viscosity, and $\dot{\gamma}$ is the shear rate. The viscosity is a measure of a liquid's resistance to flow.

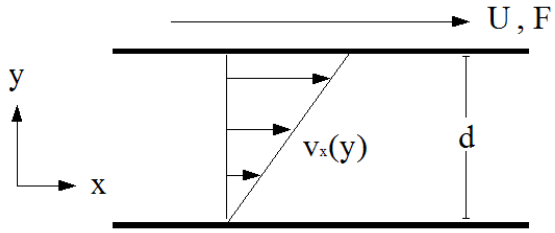

Figure 3.2: Two parallel planes with a liquid between. The upper plane moves with a velocity U, shearing the liquid

The viscosity is highly dependent on the temperature T in the liquid. The Arrhenius expression gives an approximation for this relationship for Newtonian liquids[5],

$$\eta(T) = A\mathrm{e}^{-\frac{B}{T}}, \tag{3.3}$$

where A and B are constants of the liquid. The viscosity decreases with increasing temperature. This is why it is very important to control the temperature when doing rheological measurements.

3.1.3 Non-Newtonian Liquids

Generally η is not a coefficient as suggested by Equation (3.2), but a function of the shear rate $\dot{\gamma}$. Liquids with a shear dependent viscosity are called *non-Newtonian fluids*. Liquids with a viscosity which increases with increasing shear rate are called *shear-thickening liquids*. Liquids with the opposite behavior are called *shear-thinning liquids*. Typical non-Newtonian liquids are suspensions, emulsions and polymer solutions.

3.1.4 Rheology of Suspensions

The viscosity of suspensions of solid particles in Newtonian liquids is dependent on the amount solid particles added, the particle shape and charge[6]. Einstein derived a theoretical expression for the viscosity of hard, spherical, monodisperse and non-interacting particles in a Newtonian fluid in 1906. Five years later he corrected his own calculations. The expression he found relates the viscosity, η, to the particle volume fraction, Φ, and the viscosity of the suspending medium, η_s, viz.

$$\eta = \eta_s(1 + \frac{1}{2}\Phi)(1 + \Phi + \Phi^2 + \dots)^2. \tag{3.4}$$

For sufficient dilute dispersions, neglecting higher order term of Φ, Equation (3.4) can be simplified to

$$\eta = \eta_s(1 + 2.5\Phi). \tag{3.5}$$

A considerable amount of work has been made to extend the work done by Einstein to account for effects such as particle size, shape, charge and hydrodynamic interaction between particles. The result of this work is often equations on the form[6][5]

$$\eta = \eta_s(1 + C_1\Phi + C_1\Phi^2 + \dots), \tag{3.6}$$

where $C_1 = 2.5$ and C_2 varying from 5 to 15. These expressions are only valid for dilute dispersions (less than $\Phi = 10$ %).

The influence of particle concentration of the concentrated suspensions is best determined in relation to the maximum packing fraction Φ_m[5]. The maximum packing fraction corresponds to the number of particles which gives continuous three-dimensional contact between particles throughout the suspension. In this limit flow is impossible, i.e. the viscosity tends to infinity. For monodisperse spheres Φ_m lies between[1] 0.52 and[2] 0.74. In general the maximum packing fraction is very sensitive to particle-size distribution and shape. Broader particle-size distributions have higher values of Φ_m, because small particles fit into the gaps between the bigger ones. Non-spherical particles on the other hand give lower packing fractions because of poorer space-filling.

Ball and Richmond[7] derived an expression for concentrated Newtonian suspensions by assuming that the effect of all particles added to the suspension, is the sum of the effects of particles added sequentially. By writing Equation (3.5) in a differential form and integrating the phase volume from zero to Φ, the viscosity is given by

$$\eta = \eta_s e^{2.5\Phi}. \tag{3.7}$$

[1] simple cubic
[2] face-centered cubic/hexangonal close packed

By taking into account the fact that when adding more particles to a concentrated dispersion the particles requires more space due to packing difficulties, Equation (3.7) can be modified to

$$\eta = \eta_s(1 - \mathrm{K}\Phi)^{-\frac{2.5}{\mathrm{K}}}, \tag{3.8}$$

where K is a constant less than 1.

We see that the viscosity goes to infinity when $\Phi \to \frac{1}{\mathrm{K}}$, so $\frac{1}{\mathrm{K}}$ can be identified as Φ_m. This is identical to the Krieger-Dougtherty expression[8], viz.

$$\eta = \eta_s\left(1 - \frac{\Phi}{\Phi_m}\right)^{-2.5\Phi_m}. \tag{3.9}$$

3.2 Electrorheology

The strength of the ER effect is determined by the size, shape and volume fraction of the dispersed solid particles, but the most important is the difference in conductivity and/or dielectric constant between the solid particles and the insulating oil.

There are several theoretical models to describe the microstructural of an ER fluid in an electric field. I will only give a brief presentation of the most accepted ones, namely the polarization model and the conductivity model, following Huang [9].

3.2.1 The Polarization Model

The polarization model focus on the difference in the dielectric constant between the dispersed particles and the dispersing phase. Upon application of an external electric field, each particle in the fluid is polarized due to the mismatch of dielectric constants. In general the polarization may arise from various mechanisms of charge transport, such as orientation of atomic or molecular dipoles and interfacial polarization, with the latter thought to be the most important in most cases[10].

For spherical particles with radius a and dielectric constant ϵ_p dispersed in an insulating liquid with dielectric constant ϵ_f, the induced dipole moment is given by[9]

$$\vec{p} = \frac{\epsilon_p - \epsilon_f}{\epsilon_p + 2\epsilon_f}\epsilon_f a^3 \vec{E}_{loc}, \tag{3.10}$$

where $\vec{E}_{loc}$ is the local field.

The resulting interaction between two induced spherical particles can be approximated by point dipole interaction. The interaction energy can be written as

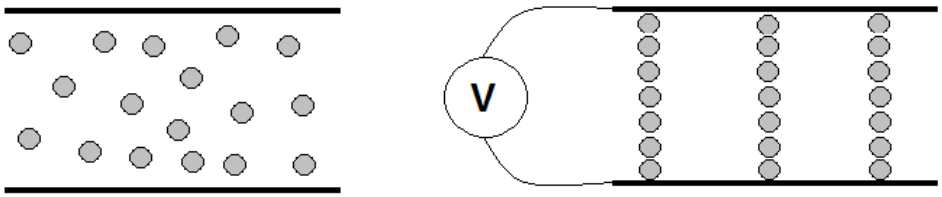

(a) (b)

Figure 3.3: Schematic illustration of micro structure change of an ER fluid before (a) and after (b) an external electric field is applied

$$W_{dip} = -\frac{\vec{p}_1 - \vec{p}_2}{r_{12}^3} + \frac{(\vec{p}_1 \cdot \vec{r}_{12})(\vec{p}_2 \cdot \vec{r}_{12})}{r_{12}^5}, \tag{3.11}$$

where $\vec{r}_{12}$ is the displacement vector from dipole $\vec{p}_1$ to $\vec{p}_2$ and r_{12} is the distance between them. The approximation holds as long as the dipoles are well separated.

The interaction between dipoles is anisotropic, making it energetic favorable to form chains aligned along the direction of the electric field. Figure 3.3 shows a schematic drawing of the chain formation. Experiments with spherical particles have shown that the ER-effect is stronger then what calculations suggests. This is because particles come very close to each other in strong electric fields, and the point dipole approximation is not valid. Multipole interactions between particles are strong and must be taken into account.

3.2.2 The Conduction Model

Anderson[11] and Lewis [12] found that the conductivity of the particle and carrier liquid plays an important role in the ER-effect when the electric field is in the low-frequency AC region or DC region. This is called the conduction model. The dipole moment for spherical particles with conductivity σ_p in a carrier fluid with conductivity σ_f is given by

$$\vec{p} = 4\pi\epsilon_f \frac{\sigma_p - \sigma_f}{\sigma_p + 2\sigma_f} a^3 \vec{E}. \tag{3.12}$$

These dipoles will also interact with each other to form chains. This model has been modified to account for increasing conductivity due to nonlinear effects in the narrow interparticle gaps[13][14].

3.2.3 Other Models

The presented models are simple physical models which only takes one parameter into consideration, namely the dielectric constant and the conductivity. They both explain why chains are formed in ER-fluids in electric fields, but they do not tell the whole story. The Maxwell-Wagner interfacial polarization model is the simplest description of particle polarization accounting for both the particle and fluid bulk conductivity, as well as their permittivities. This model has successfully described some of the main features of electrorheological response, e.g. the behavior under steady and oscillatory shear flow and time-varying electric field. In high electric fields non-linear effects are important and must be considered in the models. This has shown to be difficult.

There are a lot of theories about the role water plays in ER-fluids. The background for this is that it was observed that some ER-fluids were not active until a small amount of water was added. The double-layer-, water bridge-, interfacial polarization model are just some of the proposed theories. Since water gives limitations in the operation temperature of the ER fluid, it is generally preferred to have non-aqueous ER fluids. This is the case for the ER fluid use here. I will therefore not go further into detail on these models.

For a more extensive treatment of the theoretical models used to model the ER fluids, I recommend the review articles by Parthasarathy and Klingenberg[15] and See[10].

3.3 Flow Behavior of Electrorheological Fluids

3.3.1 Bingham Fluid Model

The flow behavior of an ER fluid in an electric field higher than E_c under shearing deformation can be represented by the Bingham fluid model. The shear stress is given by

$$\begin{aligned} \tau &= \tau_y(E) + \eta_{pl}\dot{\gamma} \ \text{ for } \ \tau > \tau_y \\ \dot{\gamma} &= 0 \ \text{ for } \ \tau < \tau_y \end{aligned} \tag{3.13}$$

where τ_y is the yield stress induced by the electric field and η_{pl} is the plastic viscosity.

The plastic viscosity will in general decrease with increasing shear rate, approaching the zero field viscosity at high shear rates. This shear-thinning behavior can be explained by a gradual degradation of the chains and the coloums in the ER fluid due to increased shearing. It is a competition between the electric field, to form new chains, and the shearing effect, to break the chains. As the shear stress increases the electric field is not able to polarize particles fast enough to form new chains, thus the decrease in the viscosity.

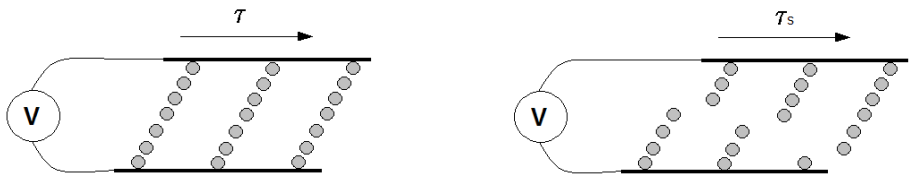

(a) (b)

Figure 3.4: Schematic illustration of the static yield stress. The chains can resist shear stress (a) up a certain limit were they break (b) and the ER fluid starts flowing

In the literature several different yield stresses occur, the *dynamic yield stress* and the *static yield stress* being the most common. The dynamic yield stress for steady shear is defined as the value of the shear stress in the limit of zero shear rate[15], i.e

$$\tau_d \equiv \lim_{\dot{\gamma}\to 0} \tau(\dot{\gamma}).$$

The static yield stress, τ_s, can be explained by the minimal stress needed to bring the sample, initially at rest, in an irreversible flow. As illustrated in Figure 3.4, the static yield stress can be interpret as the stress needed to break the chain formed in the ER fluid.

It should be noted that the yield stress can not be absolutely determined. The dynamic yield stress requires extrapolating experimental data at a finite shear rate, and thus may depend on the shear rate range employed. For the static yield stress we need to know that smaller shear stress do not induce flow at long timescales. Thus, τ_s can in general depend on the observation time.

Figure 3.5 summarizes the relation between the shear rate and the shear stress for the different liquids discussed here. The blue line shows the situation for a Newtonian liquid (η constant), the two black line shows non-Newtonian behavior ($\eta(\dot{\gamma})$) and the red line represents a Bingham fluid (η constant).

3.3.2 Static Yield Stress

Experimentally and theoretically, it is found that the static yield stress depends on the electric field and the volume fraction, Φ, of dispersed particles, viz.

$$\tau_s = \Phi^{\beta} E^{\alpha}, \tag{3.14}$$

where α and β are parameters. Experimentally, it is found that α is close to 2 for low to moderate electric field strengths and below 2 for higher field strengths. The polarization

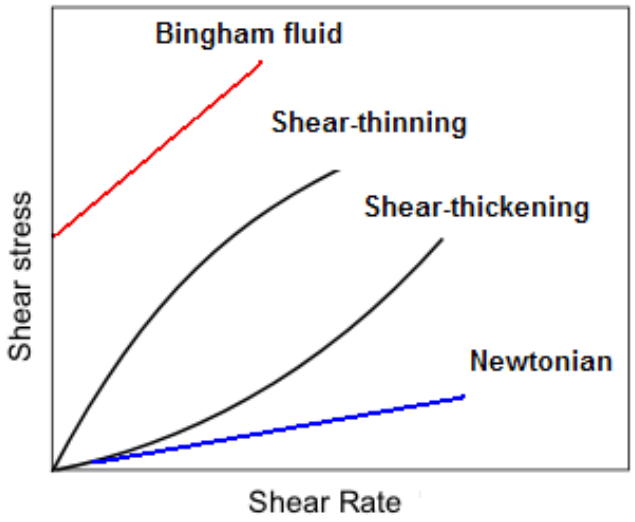

Figure 3.5: Relation between the shear stress and shear rate for different fluids

model predicts $\alpha = 2$ and $\beta = 1$ for spherical particles. The conductivity model gives $1 < \alpha < 2$, and $\beta < 1$ for high and low volume fractions and $\beta > 1$ for moderate volume fractions[1].

4 Experimental

4.1 Materials

4.1.1 Laponite

Laponite RD purchased from Laporte Ltd. was used in these experiments. Laponite is a synthetic hecorite clay, with a specific particle density of $\rho_s = 2.65$[16]. Clays are made up of sheets of tetrahedral and octahedrally coordinated cations bound to oxygen[17]. A single laponite particle consist of one octahedral sheet between two tetrahedral sheets, often referred to as a (2:1) layer clay. Smectites are one of the (2:1) clays. Smectites are so-called swelling or expanding clays, which means that they can absorb hydrated cations and polar molecules between the sheets.

Figure 4.1 shows the idealized structure for a laponite unit cell. This shows six octrahedral magnesium ions sandwiched between two layers of four tetrahedral silicon atoms. These groups are balanced by twenty oxygen atoms and four hydroxyl groups. In practice some of the magnesium ions are replaced by lithium ions and some spaces are empty, giving a charge deficiency of 0.7 per unit cell. The approximate empirical formula is $Na^+_{0.7}[Li_{0.3}Mg_{5.5}Si_8O_{20}(OH)_4]^{0.7-}$[18]. The unit cell is repeated many times in two dimensions, giving laponite a well defined shape and size, viz disc-shaped particle with a thickness of approximately 1 nm and diameter of 25-30 nm, respectively[18][19][20]. Because of this, laponite is often used as a model anisotropic colloid to study phase behavior of disk-like particles. A single laponite particle is shown in Figure 4.2.

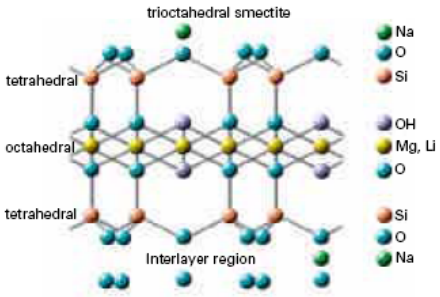

Figure 4.1: Idealized structure formula of a laponite unit cell (from [18])

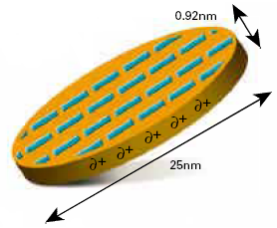

Figure 4.2: Single laponite particle (from [18])

4.1.2 Silicone Oil

The silicone oil used was Dow Corning 200 fluid 100 cS. The oil has a viscosity of 100 cS (=100 mPa·s) and a specific particle density of 0.973 at 25 °C. It is a relatively nonconducting liquid, $\sigma_f(0)$=5.0·10$^{-12}\frac{\mathrm{S}}{\mathrm{m}}$ [21].

4.1.3 Sample Preparation

Samples are prepared by heating both the laponite and the silicone oil at 130 °C for 72 hours. This is done to make sure that there is no trace of water in the samples. Immediately after the heating, the appropriate amount of laponite is mixed with 50 ml silicone oil, sealed and then cooled down to room temperature. The samples are then shaken and put in a supersonic bath for 30 minutes. Before a sample is used in rheological measurement, it must be be shaken vigorously for about 5 minutes.

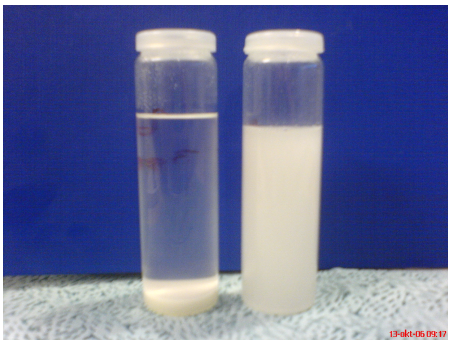

Figure 4.3: Two samples, both made of 3 g laponite and 50 ml silicon oil. The left sample has been let to rest, while the sample to the right has been shaken recently.

The samples used here were made of a varying amount of laponite, from 1 g to 15 g, dispersed in 50 ml silicone oil. The 1 g dispersion was not used for any electrorheological study, since the ER effect is very weak. The amount of laponite was weighed out before the clay was heated, so the actual amount of laponite probably was a little less because of water loss.

The concentration of suspensions are often given by the concentration by mass, χ, or the volume fraction, Φ, where

$$\chi = \frac{m_{clay}(g)}{V_{oil}(ml)} \cdot 100\%,$$

and

$$\Phi = \frac{V_{clay}}{V_{oil}} = \frac{\frac{m_{clay}}{\rho_{clay}}}{V_{oil}}.$$

The specific particle density, ρ_s, is related to the normal density, ρ, by

$$\rho_s = \frac{\rho}{\rho_{water}}, \tag{4.1}$$

where ρ_{water} is the density of water, $1.0 \cdot 10^3 \frac{\text{g}}{\text{dm}^3}$.

Table 4.1 shows the concentration of laponite in the suspensions.

Table 4.1: Concentration of suspensions used

Mass LP (g)	χ (%)	Φ
1	2	0.0075
3	6	0.023
5	10	0.038
7.5	15	0.057
10	20	0.075
12.5	25	0.094
15	30	0.113

When the laponite was dispersed in oil, no large aggregates or flocs could be seen by visual observation. Optical microscope studies performed by other however, showed large aggregates with a size distribution of 0.5 to 2 μm for the largest dimension[1].

4.2 Experimental Setup

4.2.1 Rheometer

The rheometer used is a Physica MCR 300. It is a rotational rheometer with an air bearing motor. The temperature of the sample can be controlled in a wide temperature range. All measurements performed here are taken at 25 °C, unless something else is specified. For electrorheological measurements the Electro Rheological Device (ERD) is

(a) (b)

Figure 4.4: The rheometer (a) with the ERD-system (b)

used. It consists of rotating concentric cylinder and a cup coupled to a high voltage supply, shown schematic in figure 4.5. Voltages from 0 to 12500 V can be applied. The gap between the inner and the outer cylinder is 1.13 mm and the cup contains 19.35 ml sample.

4.2.2 Rotational Viscometers

A viscometer is an instrument for measurement of shear viscosity only, while a rheometer is a instrument for measuring rheological properties in general. One can say that the rheometer is a more sophisticated and advanced version of the viscometer. It is able to produce both steady shear and oscillating motion among other things. I will give a brief introduction to how rotational concentric-cylinder viscometers work, since the priciples are the same as for the rheometer.

Rotational viscometers relay on rotation motion to achieve a simple shearing flow[5]. Inducing the flow can be done in two ways, one can either drive one member and measure the resulting couple, or apply a couple and measure the subsequent rotation rate. The former was introduced by Couette in 1888 and the latter by Searle in 1912. There are two ways that the rotation can be applied and the couple measured. The first way is to drive one member and measure the couple on the same member, or you can drive one member and measure the couple on the other.

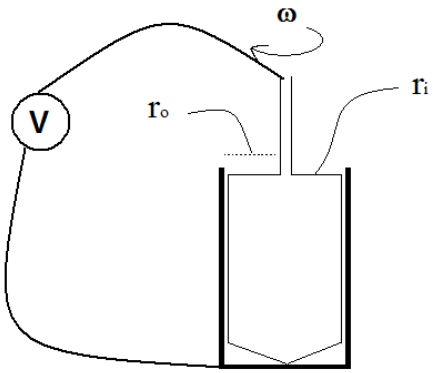

Figure 4.5: Schematic drawing of the Electro Rheological Device

Rotational concentric-cylinder viscometers consists of two parts, a rotating inner cylinder and a stationary outer cup. If the ratio between the radius of the inner and the outer cylinder is greater than 0.97, we call it a narrow-gap concentric-cylinder viscometer. If the ratio is less than 0.97 we call it a wide-gap concentric-cylinder viscometer. The latter is the case for the ERD use here, where $r_i = 13.33$ mm and $r_o = 14.46$ mm ($\frac{r_i}{r_o} = 0.92$). For the narrow-gap system the test liquid between the gap experience an almost constant shear rate and the viscosity can easily be calcualted. This is not the case for wide-gap systems. Here we need to manipulate the data to produce correct viscosity. This non-trivial operation has been done by Krieger and Maron (1954), here I will only give the results.

Wide-Gap Concentric-Cylinder Viscometer

The shear rate at the inner cylinder at a given angular velocity ω is given by[5]

$$\dot{\gamma} = \frac{2\omega}{n(1 - b^{\frac{2}{n}})}, \tag{4.2}$$

where $b = \frac{r_i}{r_o}$ and n is a parameter dependent on the test liquid.

If the couple on the cylinders is C, i.e. the force needed to rotate the cylinder at a speed ω, the shear stress in the liquid is given by

$$\tau = \frac{C}{2\pi r_i^2 L}, \tag{4.3}$$

where L is the effective immersed length of liquid being sheared.

n can be determined by plotting C vs ω on a double-logarithmic basis and taking the slope at the ω under consideration.

The viscosity can then be calculated by dividing the shear stress by the shear rate, which gives

$$\eta = \frac{Cn(1 - b^{\frac{2}{n}})}{4\pi\omega r_i^2 L}. \tag{4.4}$$

4.2.3 Motor Calibration and Viscosity Tests

Before doing rheological measurements with the Physica MCR 300 the motor speed of the rheometer may need to be adjusted. To check if this is necessary, we can rotate the the cylinder at a constant speed $n = 0.3\frac{1}{\text{min}}$ in air and plot the torque vs. time. If the resulting plot shows an uneven zigzag pattern or there are large torque fluctuations, a motor adjustment is necessary. Figure 4.6 shows a typical measurement resulting from an uncalibrated motor.

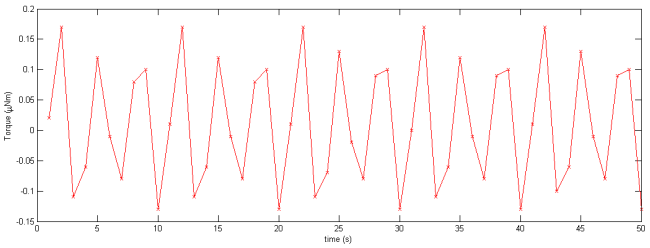

Figure 4.6: Plot of torque (μNm) vs. time (s) measured in air at constant motor speed, $n = 0.3\frac{1}{\text{min}}$, before the motor adjustment

After the motor adjustment (at $n = 0.3\frac{\text{U}}{\text{min}}$) has been performed, the air test should give a nice zigzag pattern. Such a pattern is shown in Figure 4.7. After this procedure the rheometer is ready to measure low torque ($\sim 10^{-6}$ Nm), which is necessary for measuring low-viscosity fluids.

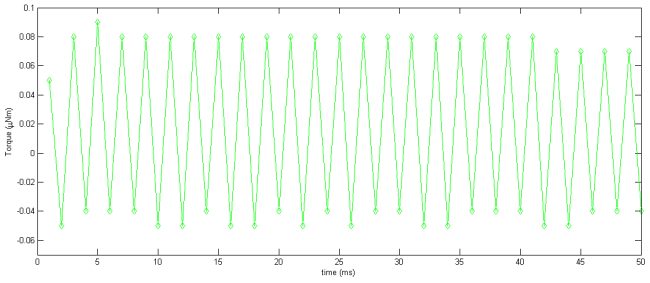

Figure 4.7: Plot of torque (μNm) vs. time (s) measured in air at constant motor speed, $n = 0.3\frac{1}{\text{min}}$, after the motor adjustment

Further viscosity measurements on two different Newtonian fluid, viz. distilled water and a viscosity standard oil, are performed to insure correct readings over a wide viscosity range. Distilled water has a viscosity less than 1 mPa·s at 25 °C, while the viscosity of the Brookfield Viscosity Standard oil used is 500 mPa·s at 25 °C. Figure 4.8 and 4.9 shows the viscosity as a function of shear rate (0.1-100 $\frac{1}{s}$) for distilled water and the Brookfield viscosity standard, respectively. We see that there are oscillations in the viscosity of water at low shear rates ($> 10\ \frac{1}{s}$). This is due to limitation in the rheometer's low torque measurement.

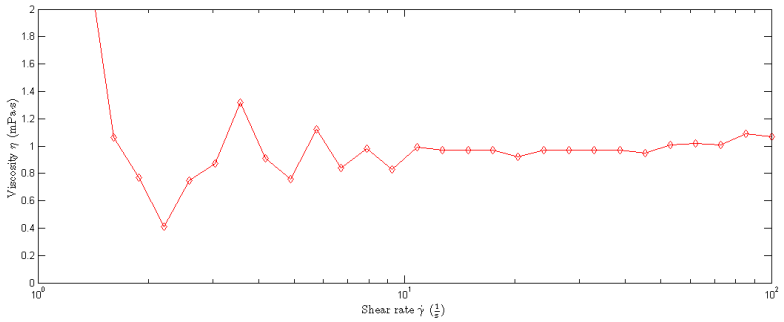

Figure 4.8: Viscosity of water vs. shear rate

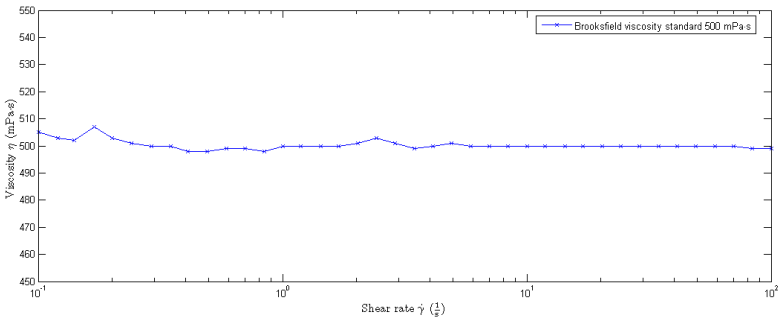

Figure 4.9: Viscosity of Brooksfield Viscosity Standard (500 mPa·s) vs. shear rate

4.2.4 Experimental Consideration Using the ERD

When applying a voltage to the ERD cell, the cup is covered by a plastic cover containing two metallic brushes, shown in Figure 4.10. These brushes touch the rotating inner cylinder, grounding the ERD cell. The metallic brushes obviously effects the rheological measurements. To check how these brushes influence the measurements several different tests are performed. First a controlled shear rate (CSR) test on distilled water was performed, $\dot{\gamma}$ increased in steps from 0.01 to 100 $\frac{1}{s}$ while measuring the viscosity. A plot

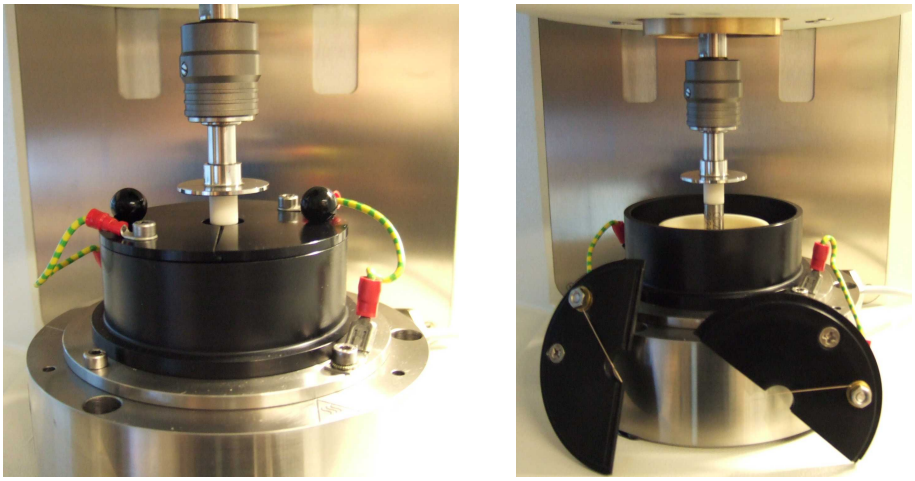

(a) (b)

Figure 4.10: The ERD with plastic cover (a) which contains two metallic grounding brushes (b) touching the rotating cylinder

of the viscosity vs. shear rate is shown in Figure 4.11, measured with and without the grounding brushes.

We see that the grounding brushes gives a huge contribution to the measured viscosity, especially at low and intermediate shear rates. Figure 4.12 shows the results of tests with constant shear rates, $\dot{\gamma}$ =10, 50, 80 and 100 $\frac{1}{s}$. The viscosity is plotted as a function of time. There are large fluctuations in the viscosity at $\dot{\gamma}$ =10 $\frac{1}{s}$, for the other the viscosity is pretty stable over the whole time period. At the higher shear rates we can find and subtract the contribution of the brushes to get the viscosity of the fluid.

A controlled shear stress (CSS) test is also carried out to see if the grounding brushes contributes to a yield stress. This is done by increasing the shear stress in steps from 0-5 Pa, while observing the change in shear rate. Figure 4.13 shows that the grounding brushes gives a contribution of $\sim$ 1 Pa to the yield stress. This value will be subtracted from all yield stress measurements.

4.3 Measurements

4.3.1 Rheological Properties of Suspensions

First thing we are interested in is the rheology of the suspensions without an electric field present. Are the suspensions Newtonian or non-Newtonian fluids, i.e. is the viscosity a function of the shear rate or is it simply a constant. This can be determined by increasing the shear rate in steps from a small value to a large, e.g. 0.01-1000 $\frac{1}{s}$, while measuring

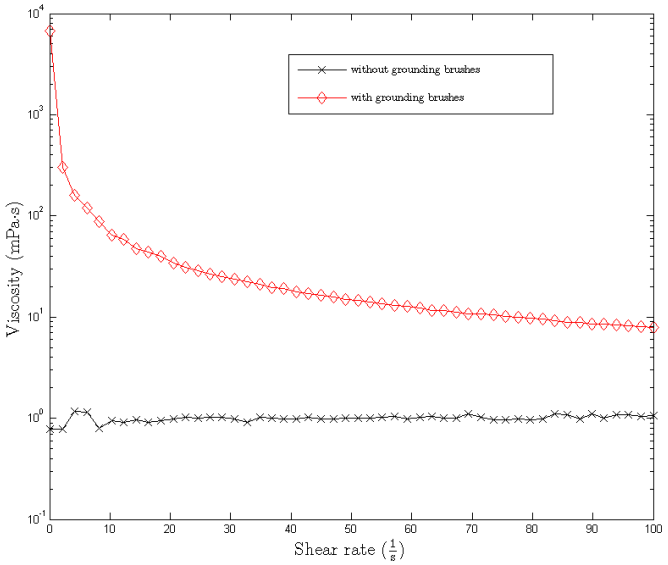

Figure 4.11: Viscosity of water vs. shear rate measured with and without the grounding brushes

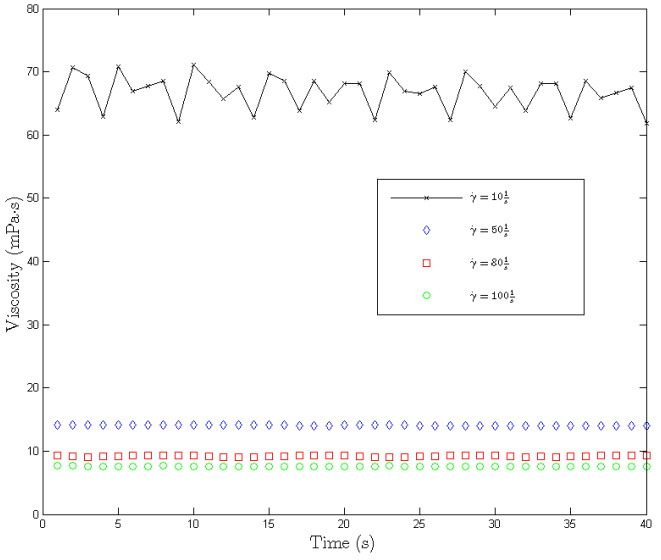

Figure 4.12: Viscosity of water vs. time measured at different shear rates with the grounding brushes

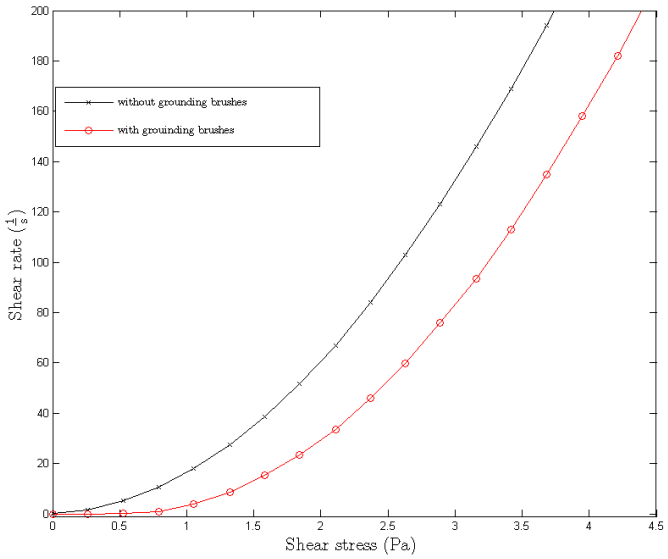

Figure 4.13: Shear stress vs. shear rate measured for water, with and without grounding brushes

the viscosity.

It is also interesting to see how the viscosity of the suspensions changes with the amount of laponite added. This can be done by measuring the viscosity of suspensions with different volume fractions. By plotting the viscosity vs. the volume fraction we can fit the data to suitable models.

Another thing that has to be considered while doing measurements is the stability of the suspensions. As seen from the two samples in Figure 4.3, the stability of the suspensions is limited due to particle sedimentation. To find out how the concentration of a samples changes over time, a controlled shear rate (CSR) test can be preformed. While shearing the suspension at a constant shear rate for a long time, e.g $\dot{\gamma}$ =10 $\frac{1}{s}$ in 40 minutes, we see how the viscosity develops over time. This makes it possible to determined how long time we can do measurement on the same sample, in order to a have approximately the same concentration of laponite in the sheared liquid.

4.3.2 Electrorheological Properties of Suspensions

The electrorheological effect can easily be observed by measuring the viscosity of the fluid in an external electric field, e.g. in a controlled shear rate test. By applying an electric field for 5 minutes to a ER suspension at res,t and then start to shear it with increasing shear rate, we expect to see a shear-thinning behavior. The time or shear

rate it takes for the ER fluid to reach its zero field viscosity can be used to characterize the strength of the ER effect. Such tests were performed in my summerjob for different suspension concentrations and electric fields. The samples I used were old and had been used many times, so the concentrations were rather inaccurate. In these measurements effects of sedimentation were not considered, neither was the effect of grounding brushes. Thus the results of these measurements will not be subject to further analysis. They are included in this report just to show the shear-thinning behavior of ER fluids in electric fields.

Measuring the static yield stress is perhaps a better way to determine the strength of the ER-effect, and it has been the main focus in my work. This is done by preshearing the suspension at $\dot{\gamma} = 100\ \frac{1}{\mathrm{s}}$ for 100 seconds, apply an electric field for 5 minutes without shearing and finally increasing the shear stress in steps from zero up to a value sufficient to break the chains, e.g. $\tau = 0 - 30$ Pa for low concentrations and $\tau = 0 - 70$ Pa for the highest concentrations.

5 Results and Analysis

5.1 Rheology of Suspensions in Zero Electric Field

5.1.1 Shear Viscosity $\eta(\dot{\gamma})$

The results of viscosity measurements for shear rate from 0.1-1000 $\frac{1}{s}$ for the suspension with the lowest and highest laponite concentration (Φ=0.023 and 0.113) are shown in Figure 5.1. Both suspensions have quite constant viscosity over the given shear rate range, i.e they behave as Newtonian fluids.

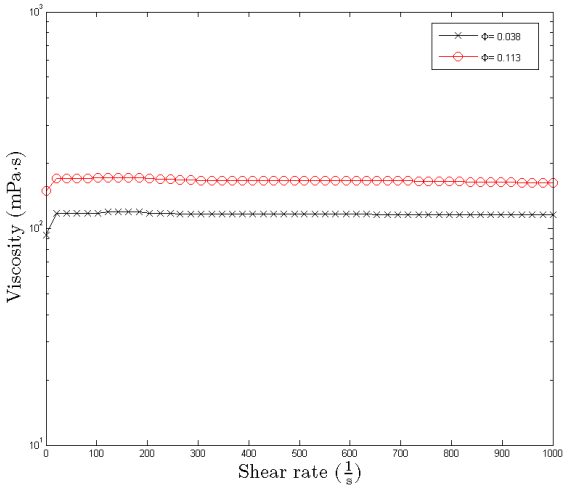

Figure 5.1: The viscosity vs. shear rate

The viscosity of the suspensions as a function of the laponite concentration is shown in Figure 5.2. The data is also fitted to the Krieger-Dougtherty expression, Equation (3.9). The fit is quite good, giving a maximum packing fraction $\Phi_m \approx 0.71$.

5.1.2 Sedimentation

Figure 5.3 shows the result of the sedimentation measurements for different laponite concentrations. There is an increase in the viscosities in the beginning, reaching a maximum

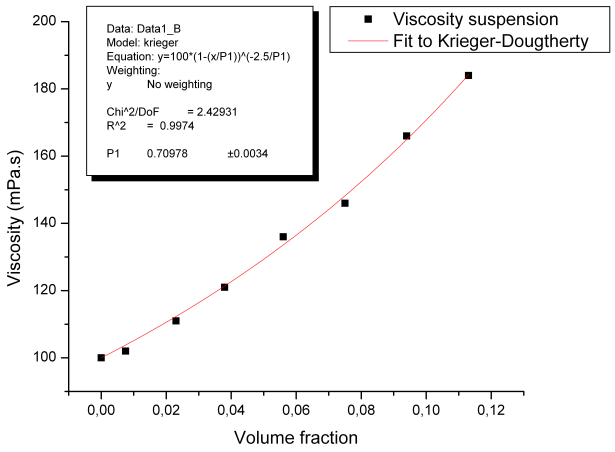

Figure 5.2: Viscosity of suspension as a function of volume fraction laponite

for $t = 250 - 450$ s, then the viscosities gradually decreases. This behavior is especially clear for the highest laponite concentrations. It is pretty obvious that the decrease in the viscosity is because particles sediment to the bottom of the cup, making the concentrations of the sheared liquid lower. The sudden increase in the viscosity is more surprising. One explanation of this behavior can be that the shearing causes laponite particles to form large aggregates, which in turn increases the viscosity. After some time the large aggregates will start sedimenting to the bottom of the cup due to gravity.

Since rheology only gives information on the macroscopic behavior of a system, we need to use other techniques to get the microscopic behavior. Suitable techniques include Small Angle Neutron Scattering (SANS) or Dynamic Light Scattering (DLS). The Physica 300 MCR Rheometer used in this study also include a Small Angle Light Scattering System which can be used during shearing. This system has not been tested yet. I am planning to set up and test this system in my Master thesis work after Christmas. Hopefully this system can give us more information about what happens in the laponite suspension under shearing. Although this can be difficult since the suspensions are opaque at high laponite concentrations.

New measurements were performed to test the reproducibility of the viscosity curves. The samples were poured back to their containers, the cup and cylinder were washed, samples were shaken and a new measurements where performed. Figure 5.4 shows the viscosity curves for a concentration $\Phi = 0.094$, for the first, second and third measurement. The shape of the curves is reproduced quite well, but the viscosity decreases for every new test. This is because every time the cup is washed some laponite is lost, giving a lower and lower concentration. The same behavior is found for all concentration. This means that to be sure that the concentration is right, we can only use a sample once.

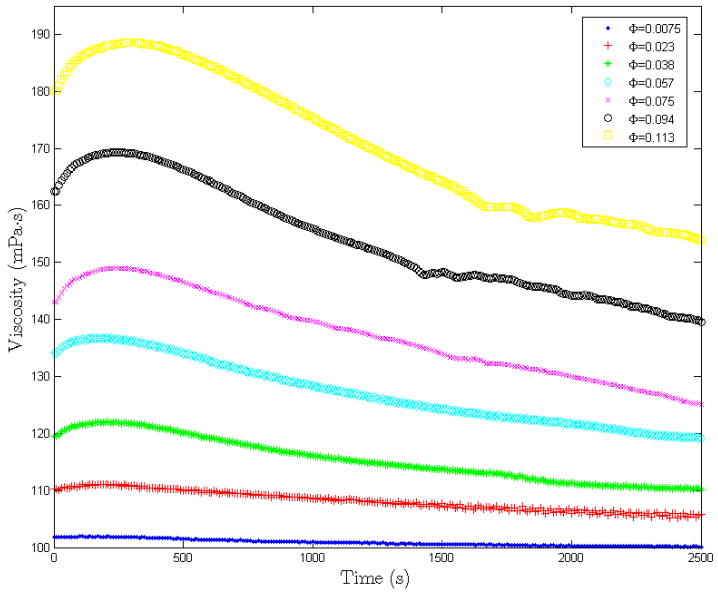

Figure 5.3: Viscosity vs. time at constant shear rate, $\dot{\gamma}$=10 $\frac{1}{\mathrm{s}}$, for different laponite concentrations

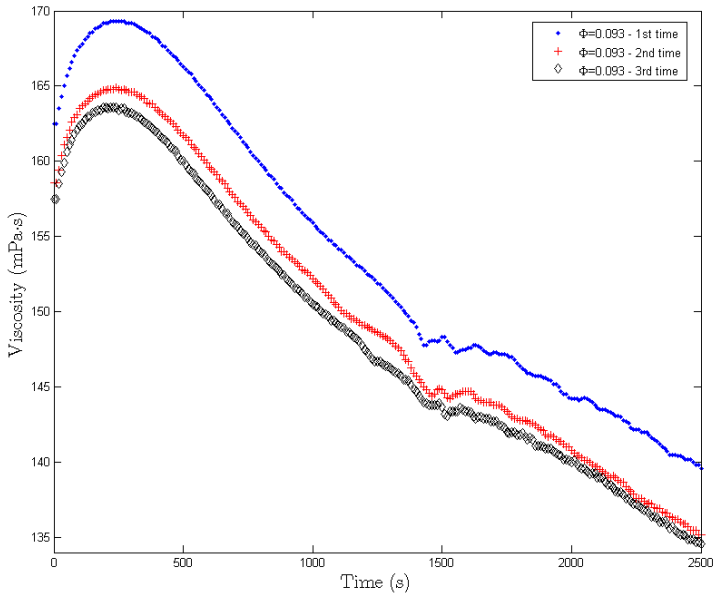

Figure 5.4: Reproducibility of viscosity curves shown for $\Phi = 0.094$

Another thing we see from Figure 5.3 is that there is a bump in the curves for the three highest concentrations. This is especially evident in figure 5.4 for $t \approx 1500$ s. A reasonable explanation for these bumps can be that the height of the sediment layer a the bottom of the cup is so big that the rotating cylinder comes in contact with it, pushing it away. This can explain why we only see this behavior for the largest concentrations.

5.2 Rheology of Suspensions in an Electric Field

5.2.1 Shear-Thinning

Figure 5.5 shows the viscosity as a function of shear rate for a $\Phi \approx 0.075$ suspension in different electric fields. The electric field was switched on for 5 minutes before the shearing start. The red dots are the viscosity in zero electric field, but with the grounding brushes. We see that the viscosity increases with increasing electric field strength, indicating the presence of more or stronger chain- or column-like structures for higher field strength. The shear-thinning behavior, due to breaking of chains or columns, is also evident. The maximum shear rate used here (100 $\frac{1}{\mathrm{s}}$) is not high enough to completely break down the structures formed in the ER fluid even at 200 $\frac{\mathrm{V}}{\mathrm{mm}}$.

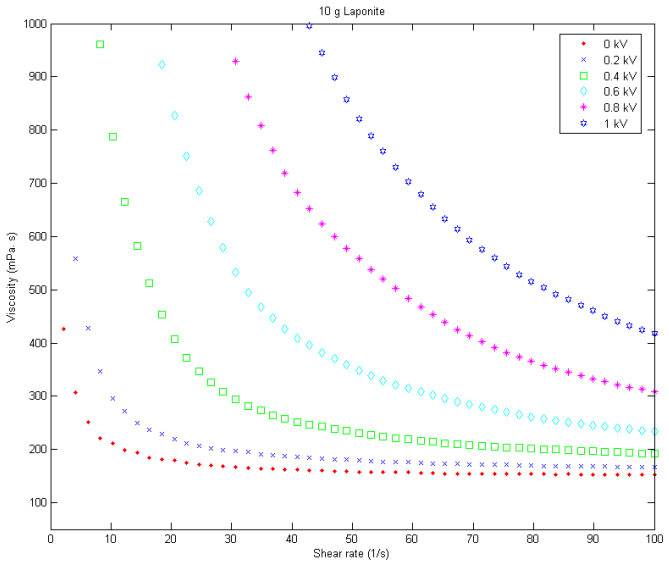

Figure 5.5: Viscosity vs. shear rate for laponite concentration $\Phi \approx 0.075$ for different electric fields

5.2.2 Static Yield Stress

Figure 5.6 and 5.7 shows the results of the static yield stress measurements for the lowest and the highest laponite concentration, respectively. In these figures the effect of the grounding brushes has not been subtracted. The value for the static yield stress corresponds to the shear stress value where there is a sudden increase in the shear rate. The static yield stress for laponite concentration of $\Phi = 0.023$ is very low, except for the highest electric field (1000 $\frac{\mathrm{V}}{\mathrm{mm}}$). For the highest laponite concentration, we see a significantly higher yield stress. Already at 400 $\frac{\mathrm{V}}{\mathrm{mm}}$ the yield stress is higher than the one measured at 800 $\frac{\mathrm{V}}{\mathrm{mm}}$ for the lowest laponite concentration.

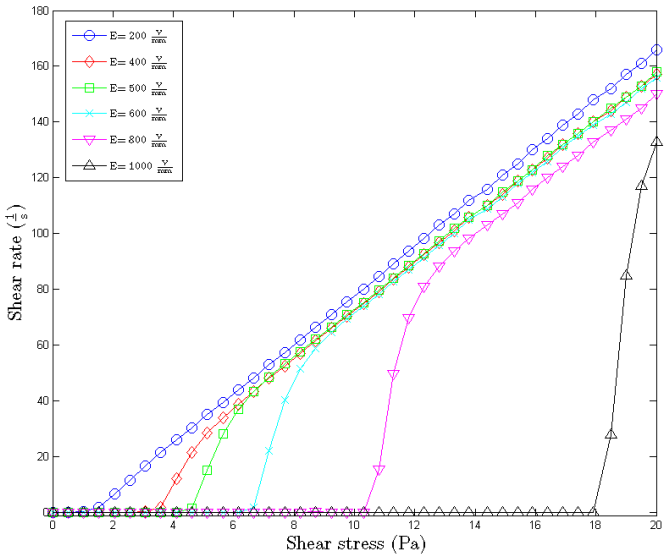

Figure 5.6: Shear rate vs. shear stress, $\Phi = 0.023$

The values for the static yield stress for all laponite concentrations are summarized in Table 5.1, where the effect of the grounding brushes has been subtracted. In Figure 5.8 the static yield stress is plotted as function of the electric field for all concentrations. We see that the ER effect is almost zero or at least very low at 200 $\frac{\mathrm{V}}{\mathrm{mm}}$, indicating that the field strength is too low to align and polarize a significant amount of laponite particles or that the process is very slow. In the 400-600 $\frac{\mathrm{V}}{\mathrm{mm}}$ range we see a clear increase in the static yield stress compared with the lowest field. This is as expected since the critical field strength, E_c, for forming chain- or column-like structures lies in this range[1]. There is a clear increase in the static yield stress from 600 to 800 $\frac{\mathrm{V}}{\mathrm{mm}}$, but the largest increase is between 800 and 1000 $\frac{\mathrm{V}}{\mathrm{mm}}$.

The plots of the static yield stress vs. the electric field, Figure 5.8, can be fitted to a allometric function form, $\tau_s = a \cdot \mathrm{E}^{\alpha}$, to get the electric field dependency of the yield

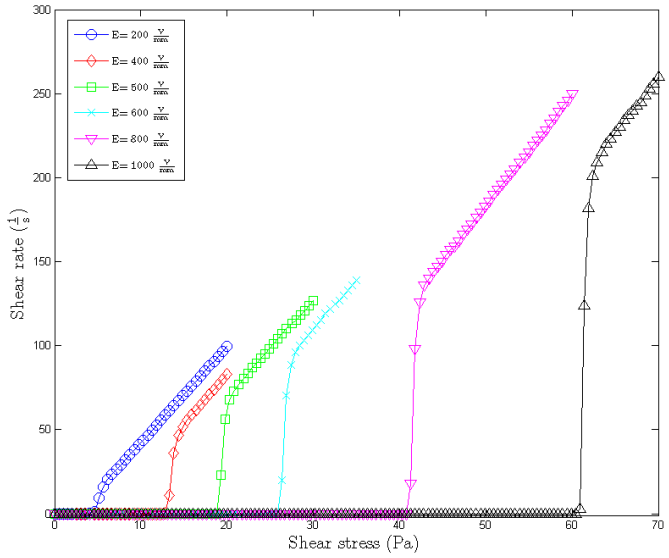

Figure 5.7: Shear rate vs. shear stress, $\Phi = 0.113$

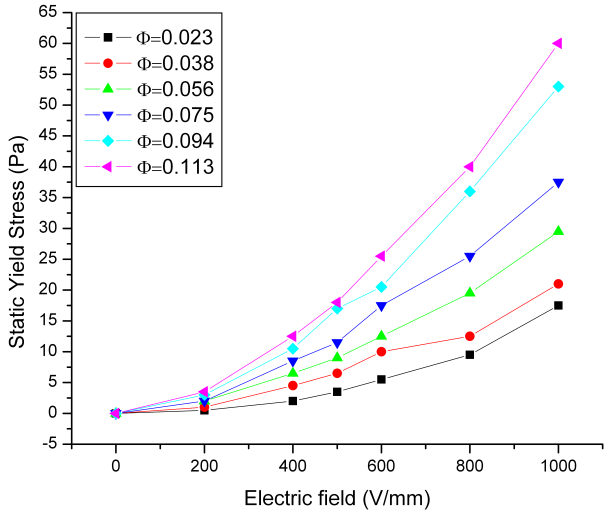

Figure 5.8: Static yield stress vs. E for different laponite concentrations

Table 5.1: Static yield stress for different laponite concentrations in electric fields from 0.2-1 $\frac{\text{kV}}{\text{mm}}$

E ($\frac{\text{V}}{\text{mm}}$)	Φ=0.023 (Pa)	Φ=0.038 (Pa)	Φ=0.058 (Pa)	Φ=0.075 (Pa)	Φ=0.094 (Pa)	Φ=0.113 (Pa)
200	0.5	1.0	2.0	2.0	3.0	3.5
400	2.0	4.5	6.5	8.5	10.5	12.5
500	3.5	6.5	9.0	11.5	17.0	18.0
600	5.5	10.0	12.5	17.5	20.5	25.5
800	9.5	12.5	19.0	25.5	36.0	40.0
1000	17.5	21.0	29.5	37.5	53.0	60.0

stress. Figure 5.2.2 shows the fit for the largest laponite concentration and the parameters obtained by the fitting. The other plots were also fitted to the same function form. The electric field dependent parameters α obtained by the fitting procedure are shown in Table 5.2.

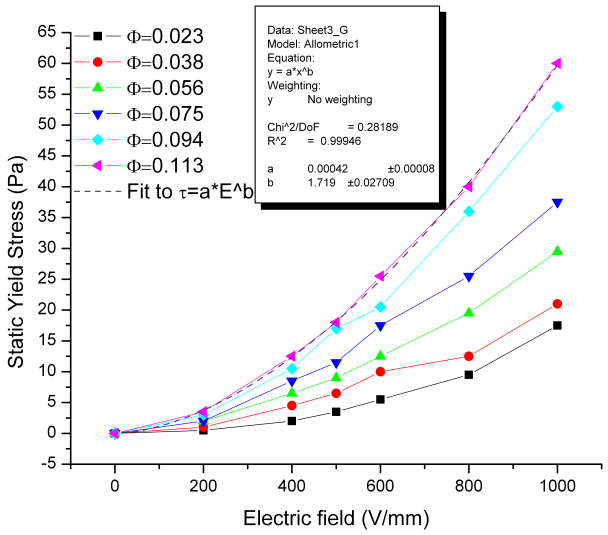

To get Φ^β we plot the static yield stress as a function of the volume fraction for different electric fields and use the same fitting procedure as above. This is shown in Figure 5.9, where E=600 $\frac{\text{V}}{\text{mm}}$ has been fitted to $\tau_s = a \cdot \Phi^\beta$. It seems to be an almost linear dependence between the static yield stress and the volume fraction. This is confirmed by the fitting procedure, which gives β between 0.91 and 1.07, as shown in Table 5.3.

We see that the electric field dependent parameter (Table 5.2), α, for the lowest laponite concentration ($\alpha = 2.37$) differ significantly from the others ($\alpha \sim 1.70$). The reason for

Table 5.2: Parameter obtained by fitting $\tau_s \propto E^{\alpha}$

Volume fraction Φ	E^{α} α
0.023	2.37±0.10
0.038	1.66±0.15
0.054	1.69±0.04
0.075	1.63±0.06
0.094	1.75±0.05
0.113	1.72±0.03

Table 5.3: Parameter obtained by fitting $\tau_s \propto \Phi^{\beta}$

Electric field $\frac{\mathrm{V}}{\mathrm{mm}}$	Φ^{β} β
200	1.07±0.06
400	0.98±0.05
500	1.00±0.09
600	0.91±0.04
800	1.01±0.07
1000	0.92±0.08

this can be that the ER effect is very small up until the highest electric fields (800, 1000 $\frac{\mathrm{kV}}{\mathrm{mm}}$), thus giving a larger field dependence. The average value of α is 1.80.

The average value of β (Table 5.3) is 0.98. This gives an linear relationship between the static yield stress and the volume fraction, as predicted by the polarization model.

The results for the α parameter are in fairly good agreement with what PhD. K.P.S Palmar found in his PhD thesis[1]. He got α-values between 1.72 and 1.94 with a average of 1.85 for higher electric fields (1.1-3.54 $\frac{\mathrm{kV}}{\mathrm{mm}}$) and concentrations Φ from 0.179 to 0.488. However, it seems like he has used the concentration by mass χ or something else instead of the volume fraction. If we compare the viscosity he got for a 0.45 volume fraction solution with what I got for a 0.113 volume fraction solution, we see that we get approxmately the same viscosity, i.e. $\sim$ 180 mPa·s. This means that one of us has calculated the volume fraction wrong, and the value he obtained for β, 1.70, is probably wrong.

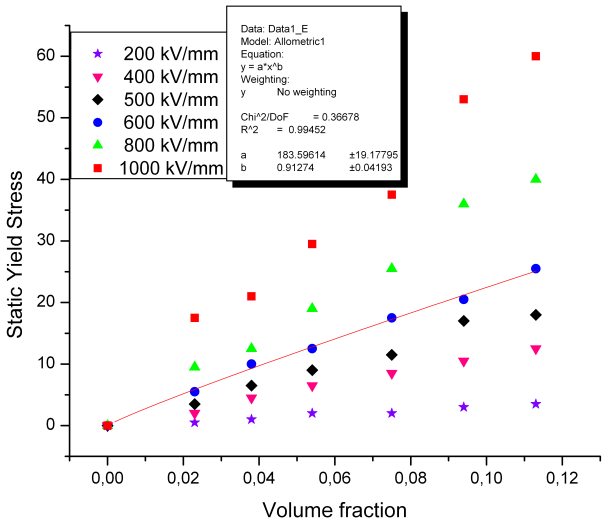

Figure 5.9: Static yield stress vs. volume fraction for different electric field

6 Conclusion

I have discussed different things that have to be considered when using the Electro Rheological Device on the rheometer. The grounding brushes gives a large contribution to the viscosity especially at low shear rates. At low shear rates there are also large fluctuations in the viscosity contribution from the brushes which makes accurate measurements difficult. At higher shear rates the brushes gives an almost uniform contribution which can easily can be subtracted in order to get the viscosity of the liquid. The grounding brushes also contributes to a artificial yield stress in the order of 1 Pa.

The dispersions of laponite in silicone oil with volume fraction up to 0.113 behaves as Newtonian liquids in the shear rate range investigated, 0-1000 $\frac{1}{\mathrm{s}}$. The viscosity of the disperions as function of volume fraction laponite added was fitted to the Krieger-Dougtherty expression. The maximum packing fraction was determined from the fitting procedure, which gave $\Phi_m = 0.71$.

Sedimentation tests were performed to check the stability of the dispersions due to sedimentation. It was found that the viscosity first increases to a maximum and then gradually decreases. The increase is maybe due to changes in the particle size as a consequence of shearing, i.e. formation of large aggregates etc. The decrease in the viscosity occures because particles sediment to the bottom of the container, decreasing the overall concentration of the sheared dispersion.

When the laponite dispersions are under influence of an electric field higher than $\sim$600 $\frac{\mathrm{V}}{\mathrm{mm}}$ the viscosity of the dispersion increases dramatically. This behavior characterizes Electrorheological fluids. The increase in the viscosity is a result of polarized particles forming chain- or column-like structure in the direction of the electric field. This formation also gives ER fluids a yield stress. The static yield stress, the stress needed to break the structure in an ER fluid initially at rest, was measured. It was found that the static yield stress depends on the volume fraction and the electric field according to $\tau_s = \Phi^\beta \cdot E^\alpha$, where β was close to 1 and α was around 1.70, except for the lowest concentration where $\alpha = 2.37$. The average value of β and α was 0.98 and 1.80, respectively. The α value is close to what PhD. K.P.S Palmar found in his thesis, 1.85. The β value he got, 1.70, differs from the result obtained here.

Part II

Modified Laponite

7 Surface Modification of Laponite

7.1 Aim

To prevent laponite particles from forming large aggregates when dispersed in oil, we want to try to alter the nature of the clay surfaces. One idea was to try to make the surfaces hydrophobic, or actually lipophilic. A lipophilic molecule will attract non-polar organic compounds such as oils. Thus lipophilic molecules in oil will maximize their contact with the non-polar phase and disperse as single molecules. Changing the surface properties of laponite can be done by exchanging the Na^+ ions on the laponite surface with other cations with the desired properties.

7.2 Clays in Water and Cation Exchange

A very important property of clay surfaces is their chemical activity and their interaction with ions in aqueous solution[17]. In these solutions we usually find dissolved species such as charged ions or molecules. Some of these ions or molecules can be attracted to the charged clay surfaces and *adsorbed* onto the surface. In some species of clay charged ions and molecules can be *absorbed* by the clays into internal crystallographic sites. The adsorbed ions are normally accompanied by water molecules, expanding the clays, in aqueous solution.

If more then one type of ion or charged molecule can be adsorbed to the clay surfaces, a selection process will start. The amount of adsorbed ions or molecules on the clay surfaces depends on the concentration of each kind. The more an ion or molecule is present in the solution, the more of it will be on the clays surface. The attraction of ions or charged molecules are not the same for all species. There is also a selection between different types of ions, i.e. some ion-types are more attracted to the clay surface then others. This depends on the chemical constitution of the clay, as well as the affinity of the ions or molecules present in the aqueous solution. The composition of the aqueous solution, i.e. the concentrations of ions in solution, can affect the attraction for clay sites as well. If an ion that is adsorbed or absorbed by the clay is displaced by another due to a change in the aqueous solution, the ion is *desorbed*. However, if the desorbed ion instead is replaced by another ion, the ion is exchanged. This process is called ion exchange. For simple ionic species in solution, these relations are known as *cation exchange*.

A measurement for the total number of charged ions which can be fixed onto the surfaces of clays is given by the *cation exchange capacity* (CEC). The CEC gives the number of moles of ionic charge fixed on a given amount of dry clay, usually 100 g. The values are expressed in milli-equivalents of charge (moles) divided 100 g clay. The reason for this strange measurement is that such values are often determined for bulk clay or soil samples where one has a mixture of clay and other phases present.

7.3 Quaternary Ammonium Surfactants

In the literature it has been reported that by treating clays with quaternary ammonium surfactants the clay surfaces has become hydrophobic[22][23][24]. The procedure often used, is to add quaternary ammonium surfactants to dilute (e.g. wt. 1 %) aqueous solutions of clays while stirring and heating the solution. The added amount of surfactant is based upon the CEC. Nakamura and Thomas[22] reported that a concentration of CTAB corresponding to 2×CEC of the clay was used to achieve hydrophobic surfaces on the clay, but also 1×CEC has been used[24].

Quaternary ammonium surfactants, e.g. cetyltrimethylammonium bromid (CTAB), dimethyl dioctadecyl ammonium bromid (DODAB), cetyltrimethyl ammonium chloride (CTAC), cetyltrimethylammonium acetate (CTAA) etc., are amphiphilic molecules, i.e. chain like molecules with a hydrophilic head group and hydrophobic tail. The structural formula is NR_4^+, with R being alkyl groups. When these molecules are dispersed in aqueous solutions over a certain concentration they can form micelles. Micelles are aggregates of amphiphilic molecules, formed in such a way that the contact between the the hydrophobic tails and water is minimized.

When a quaternary ammonium surfactant is added to a water/clay solution the charge balancing cations (Na^+ for laponite) on the clay surfaces will be exchange by CTA^+. ions. This is because of the propensity of the ions and the fact that the hydrophobic tail prefers to hide from the aqueous medium. If the amount of CTA^+ ions present in the solution is right a complete cation exchange is possible.

7.4 Cation Exchange Using CTAB

In our attempt to alter the clay surfaces we used CTAB, simply because it was available from our supplier, VWR. The chemical structure of CTAB is shown i Figure 7.1. The molar mass of CTAB is $M_m = 346.46\ \frac{\text{g}}{\text{mole}}$.

The first procedure we tried was to mix the appropriate amount CTAB to a 1 wt. % solution of laponite in water while strirring and heating the solution. Then we simply boiled away the water. The remaining powder was then crushed with a pestle and mortar and then dispersed in silicone oil. The resulting dispersion showed large white aggregates.

We realized that with this procedure CTAB molecules who had not reacted with laponite would still be present in the powder.

The second procedure we tried is similar to what Leach et al.[25] used, only that they used the surfactant DODAB. We decided to try with a CTAB concentration corresponding to 2×CEC of laponite.

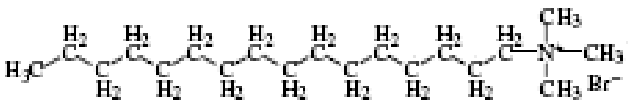

Figure 7.1: Chemical structure of CTAB (from [26])

Several different CEC values for laponite are reported in the literature, from 47[27][28] to 75[24][29] $\frac{\text{mequiv}}{100\text{g}}$. We decided to use the CEC value of 47 $\frac{\text{meq}}{100\text{g}}$ after consulting with supervisor Fossum. For monovalent ions[1] 1 meq equals 1 milli mole[30].

For every gram laponite we should then add (using 2× CEC) x grams of CTAB,

$$x = 2 \times \text{CEC} \cdot M_{m(\text{CTAB})} = \frac{0.094\ [\text{mole CTAB}]}{100\ [\text{g laponite}]} \cdot M_{m(\text{CTAB})} \frac{[\text{g}]}{[\text{mole}]}$$
$$= 0.3256 \frac{[\text{g CTAB}]}{[\text{g laponite}]}.$$

The procedure used to prepare CTAB modified Laponite:

1. Mix 2.5 g CTAB in 400 ml distilled water while stirring and heat up to 80 °C
2. While stirring and heating the solution add 100 ml ethanol (20 %)
3. Add the stoichiometric amount of laponite (7.67 g) to the hot solution
4. Cover and cool the stirring solution to room temperature over night
5. Filtrate the solution using 0.2 μm filterpaper
6. Redisperse the the CTAB/laponite in a 125 ml (50:50) ethanol/water solution
7. Repeat the filtering process four times
8. Dry the CTAB/laponite in 100 °C over night
9. Crush powder with pestle and mortar
10. Dry powder one hour at 100 °C

[1] Monovalent ion: one valence

11. Put the powder in an airtight container

The solubility of CTAB in water was 3 $\frac{g}{L}$. We used higher CTAB concentration which resulted in formation of flocs in the solution. By adding ethanol to the water solution CTAB dissolved better, thus making it more reactive. This procedure gave about 7 g dry CTAB modified Laponite.

7.5 Rheological Measurements

Before the CTAB modified laponite was dispersed in silicone oil, the clay and the silicone oil was heated at 130 °C over night to remove remaining water. This treatment seemed to affect the modified clay, because when mixing the clay and the oil together the solution got yellow and many large particles was observed. Visual sedimentation test showed that the dispersion was not very stable. Measurements with the rheometer showed the same. In Figure 7.2 the sedimentation curve for the CTAB modified laponite is compared with the same concentration of pure laponite. The viscosity of the dispersion of modified clay is about 15 mPa·s smaller then pure laponite suspension initially, which may be because large particles sediment very quick. The overall shape of the curves is however much the same, with an increase in the beginning, followed by a gradual decrease.

A static yield test was performed on the CTAB modified laponite in an electric field of 1 $\frac{kV}{mm}$, shown in Figure 7.3. The modified clay showed a much weaker static yield stress, $\sim$ 16 Pa, compared with pure laponite at the same concentration $\Phi = 0.075$, which has 37.5 Pa. This can be explained by the fact that the relative laponite concentration is lower for the CTAB modified laponite then the pure laponite, and the rapid particle sedimentation. It is also possible that the heating treatment destroyed the modified clay. The viscosity shows a strange behavior over the static yield stress.

The remaining CTAB modified laponite ($\sim$0.3 g) was dispersed in a small amount of silicon oil ($\sim$5 ml), $\Phi \approx 0.023$, without heating the clay. The clay dispersed quite well, but also this dispersion contained large particles visible for the eye. This indicate that the crushing procedure we used were insufficient.

7.6 Industrial Treated Laponite

An industrial treated laponite from Southern Clay Products was also tested. The chemical product identification name is Alkyl Quaternary Ammonium Smectite (AQAS) and the trade name SCPX-2849, SO-8147. No further information on the product was available.

The AQAS clay was dispersed in silicon oil following the same procedure described for pure laponite. Two dispersions were made, one with volume fraction $\Phi = 0.038$ and one with $\Phi = 0.057$. These dispersions were much more stable then the dispersions of

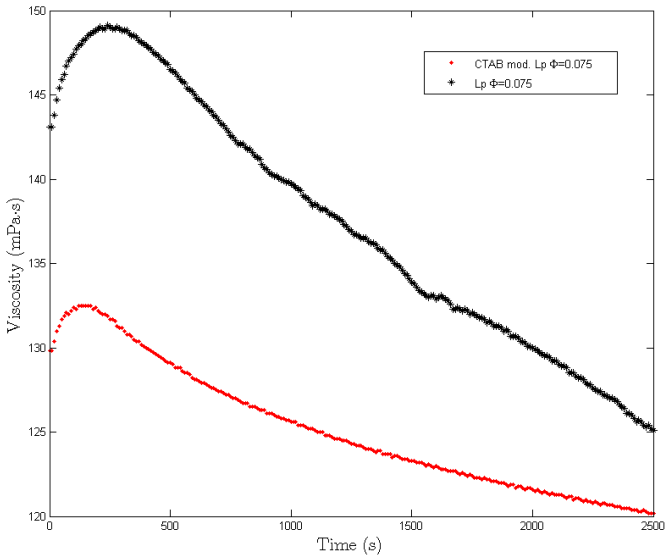

Figure 7.2: Viscosity vs. time at constant shear rate $\dot{\gamma}$=10 $\frac{1}{\mathrm{s}}$

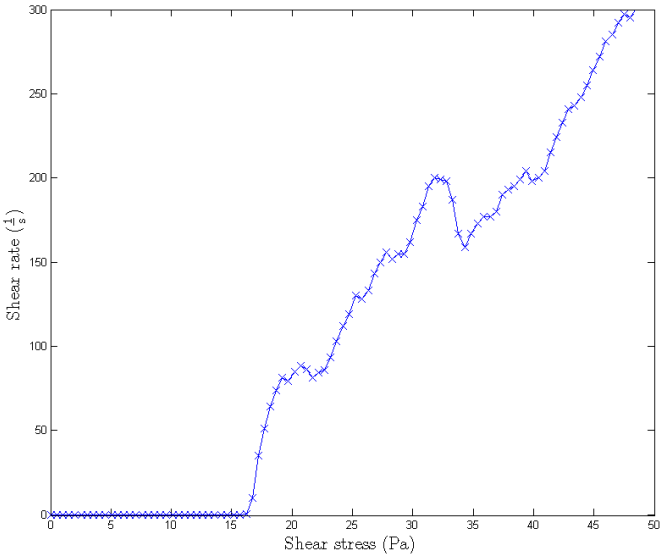

Figure 7.3: Static yield stress measurement of CTAB mod. laponite (Φ = 0.075) in 1 $\frac{\mathrm{kV}}{\mathrm{mm}}$

pure laponite in silicone oil. Sedimentation tests done with the rheometer also confirmed this. The results are shown in Figure 7.4. For the lowest concentration we see a gradual increase in the viscosity over the whole time period from 142 to 145.5 mPa·s. While the highest concentration there is a increase in the viscosity up to t≈800 s, followed by a flat region up to t≈1800 s, from this point there is a slow decrease in the viscosity.

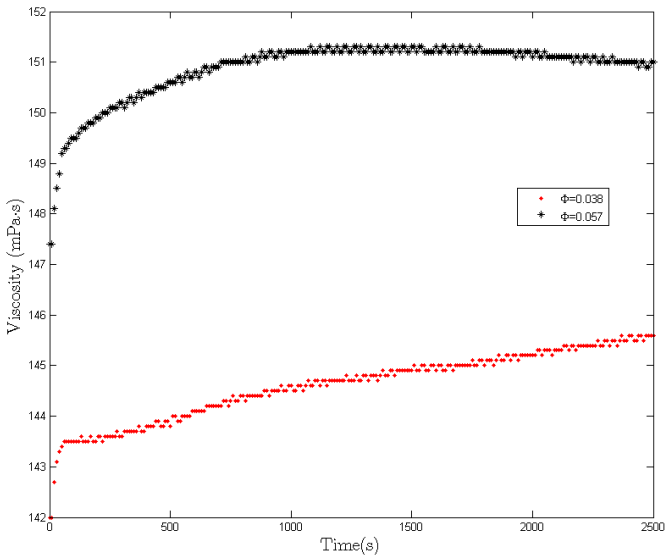

Figure 7.4: Viscosity vs. time for modified laponite at $\dot{\gamma}$=10 $\frac{1}{\mathrm{s}}$

To test the ER effect of the AQAS clay, static yield stress tests were performed in the same way as described before. A field strength of 1 $\frac{\mathrm{kV}}{\mathrm{mm}}$ was used. The result of these measurements is shown i Figure 7.5. The static yield stress is about 5 Pa for $\Phi = 0.038$ and 11 Pa for $\Phi = 0.057$. This is about four and three times lower then the static yield stress measured on the normal laponite suspension at the same concentrations and electric field.

7.7 Conclusion

Whether or not the surface treatment of laponite was successful is unknown. Hardly any conclusions can be made of the CTAB modified laponite dispersed in silicone oil, since the heating treatment may have destroyed the clay. Unfortunately there were not enough CTAB modified clay left to do new tests in the rheometer or enough time to make a new modified clay. The small sample we made showed some promising properties, even though there were large particles present. The crushing of the CTAB modified clay were insufficient, and must be improved. So new tests have to be done next year.

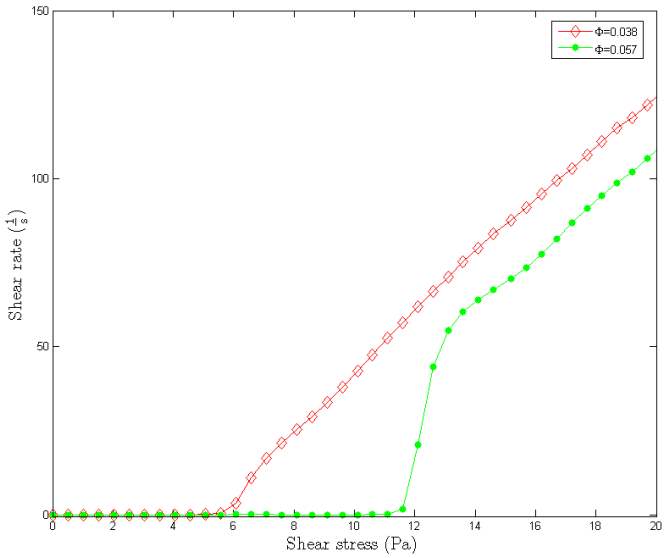

Figure 7.5: Static yield stress test for the AQAS clay at 1 $\frac{\text{kV}}{\text{mm}}$

The results of the sedimentation tests for the AQAS clay dispsersed in silicone oil were very good. The viscosities did not decrease over the time period, they rather increased a bit. This is a completely different behavior than for the normal laponite suspensions. However, the static yield stress measured for the two concentrations was three to four times weaker than for the normal laponite suspensions. One reason for this is that the relative laponite concentration are much smaller in the AQAS clay. It should be possible to use higher concentration of this clay since it is more stable to achieve the same ER effect.

Bibliography

[1] K.P.S Parmar. *Electrorheological suspensions of laponite in oil: rheometry studies under steady shear.* PhD thesis, NTNU, 2006.

[2] W.M. Winslow. Induced Fibration of Suspensions. *J. Appl. Phys.*, (**20**):1137–1140, 1949.

[3] T. Hao. Electrorheological Fluids (review). *Adv. Mater.*, 13(**24**):1848–1857, 2001.

[4] R.C. Kanu and M.T Shaw. Enhanced Electrorheological Fluids Using Anisotropic Particles. *J. Rheol.*, 42:657–670, 1998.

[5] J.F. Hutton H.A. Barnes and K. Walters. *An Introduction to Rheology.* Elsevier, 1989.

[6] P.C Mørk. *Overflate og Kolloidkjemi.* NTNU, 2004.

[7] R. Ball and P. Richmond. Dynamics of Colloid Dispersion. *J. Phys. Chem. Liquids*, (**9**):99–116, 1980.

[8] I.M. Krieger and T.J. Dougherty. A Mechanism of Non-linear Flow in Suspensions of Rigid Spheres. *Trans. Soc. Rheol.*, (**3**):137–152, 1959.

[9] XianXiang Huang. *Theoretical Study of Electrorheological Fluids.* PhD thesis, Hong Kong University of Science and Techology, 2004.

[10] H. See. Advances in Modelling the Mechanisms and Rheology of Electrorheological Fluids. review. *Kor-Aust. Rheo. J.*, 11(**3**):169–195, 1999.

[11] R.A. Anderson. Effect on Finite Conductivity in Electrorheological Fluids. In R. Tao, editor, *Int. Conf. on Electrorheological fluids: mechanisms, properties, structure and applications*, pages 81–90, Carbondale, Illinois, USA, Oct. 15-16, 1991. 1992. World Scientific.

[12] L.C. Davis. Finite-Element Analysis of Particle-Particle Forces in Electrorheological Fluids. *Appl. Phys. Lett.*, **60**(3):319–312, 1992.

[13] N. Felici et al. A Conduction Model of Electrorheological Fluids. In R. Tao and G.D. Roy, editors, *Int. Conf. on Electrorheological fluids: mechanisms, properties, structure and applications*, pages 139–152, Feldkirch, Austria, July 20-23, 1993. 1994. World Scientific.

[14] J.N Foule and N. Felici. Microscopic Model of Interactions between Particles in an Electrorheological Fluid. *J. Electost.*, 33:103–112, 1994.

[15] M. Parthasarathy and D.J. Klingenberg. Electrorheology: Mechanisms and Models. review. *Mat. Sci. Eng.*, R17:57–103, 1996.

[16] L. Jyotsana. Interaction of Polymer with Clays. *J. Appl. Cryst.*, 33:673–676, 2000.

[17] Bruce Velde. *Origin and Mineralogy of Clays.* Springer, 1995.

[18] Laponite.com. Brochure. http://www.laponite.com/pdfs/laponite.pdf (30.Oct 2006).

[19] M. Kroon et al. Structure and Formation of a Gel of Colloidal Disks. *Langmuir*, 57 (**2**):1962–1971, 1998.

[20] S. Bhatia et al. Scattering of Disklike Particle Suspensions: Evidence for Repulsive Interactions and Large Length Scale Structure from Static Light Scattering and Ultra-Small-Angle Neutron Scattering. *Langmuir*, 19(**3**):532–535, 2003.

[21] C.W. Wuy and H. Conrad. The Temperature Dependence of the Conductivity of Silicone Oil and Related Electrorheology of Suspensions Containing Zeolite Particles. *J. Appl. Phys.*, (**31**):3403, 1998.

[22] T. Nakamura and J.K. Thomas. Formation of Surfactant Double Layers on Laponite Clay Colloids. *Langmuir*, (**3**):234–239, 1987.

[23] R.A. DellaGuardia and J.K. Thomas. Photoprocesses on Colloidal Clay Systems. 2. Quenching Studies and the Effect of Surfactants on the Luminescent Properties of Pyrene Derivatives Adsorbed on Clay Colloids. *J. Phys. Chem.*, (**87**):3550–3557, 1983.

[24] H.J.M. Hanley et al. Surfactant Adsorption on a Clay Mineral: Application of Radiation Scattering. *Langmuir*, (**20**):5276–5282, 1997.

[25] E.S.H Leach et al. Nonaqueous Suspensions of Laponite and Montmorillonite. *Langmuir*, (**21**):3821–3830, 2005.

[26] S. V. Kharlamov et al. Aggregation in a Mixture of Cetyltrimethylammonium Bromide and Polyoxyethylene 600 Monolaurate Solutions. *Colloid Journal*, 68(**4**):550–557, 2006.

[27] D. Borden and R.F. Giese. Baseline Studies of the Clay Minerals Society Source Clays: Cation Exchange Capacity Measurements by the Ammonia-Electrode Method. *Clays and Clay minerals*, (**5**):444–445, 2001.

[28] P.D. Kaviratna et al. Dielectric Properties of Smectite Clays. *J. Phys. Chem Solids*, (**12**):1897–1906, 1995.

[29] H.J.M. Hanley et al. Surface Adsorption in a Surfactant/Clay Mineral Solution. *Int. J. Therm.*, (**4**):1155–1164, 1998.

[30] Wikipedia. Equivalent. http://en.wikipedia.org/wiki/Meq (Oct. 2006).